Reducing the optical end losses of a linear Fresnel reflector using novel techniques

Evangelos Bellos[1], Christos Tzivanidis[1], M.A. Moghimi[2]

[1]Thermal Department, School of Mechanical Engineering, National Technical University of Athens, Zografou, Heroon Polytechniou 9, 15780 Athens, Greece

[2] Clean Energy Research Group, Department of Mechanical and Aeronautical Engineering, University of Pretoria, Pretoria, South Africa

Corresponding author: Evangelos Bellos (bellose@central.ntua.gr)

Highlights

• Various ideas for the optical enhancement of a linear Fresnel collector are studied.

• The results are evaluated on a yearly basis for the climate of Athens – Greece.

• The use of an extended receiver enhances the yearly performance up to 50.3%.

• The use of a displaced receiver enhances the yearly performance up to 20.2%.

• The combination of these methods enhances the yearly performance up to 48.7%.

Abstract

The objective of this work is the investigation of some alternative ideas for enhancing the optical performance of a linear Fresnel reflector (LFR) with North-South orientation. More specifically, the examined methods aim to reduce the optical end losses which are crucial for the short LFR plants in particular during the winter period. The first studied idea is the extension of the receiver after the concentrator which is able to enhance the yearly mean incident angle modifier up to 50.3%. The second examined idea is the displacement of the receiver in order to eliminate the non-illuminated area at the beginning of the receiver. This idea proved that the mean yearly incident angle modifier can be enhanced up it 20.2% for a displacement equal to 20% of the concentrator length. The third examined idea is the hybrid design with the extended and displayed receiver in combined. This idea leads to intermediates enhancements compared to the previous cases but its advantage is the lower investment cost compared to the simple receiver extension case. The analysis is performed with a developed optical model in SolidWorks Flow Simulation and the yearly evaluation has been done for the location of Athens (Greece).

Keywords

Linear Fresnel reflector, Optical efficiency, Optical end losses, Receiver displacement, Receiver length, Optimization

1. Introduction

Solar energy utilization is a vital weapon for facing important energy problems such as fossil fuel depletion, global warming and the increasing price of electricity [Myers and Goswami, 2016; Tiwari and Tiwari, 2016]. Solar concentrating power is the major solar technology for producing useful heat for various applications such as power production, refrigeration, industrial heat and desalination [Zhou et al., 2017; Loni et al., 2016]. The most usual solar concentrating technologies are the parabolic trough solar collector (PTC), the linear Fresnel reflector (LFR) and the solar tower [Qiu et al., 2017; Montes et al., 2017]. Among them, the LFR is a developing technology which is improved year by year and it has the potential for low-cost heat production [Desai and Bandyopadhyay, 2017]. However, the LFR suffers from reduced thermal efficiency due to the high optical losses [Bellos et al., 2016].

An LFR consists of discrete primary linear mirrors which are located close to the ground [Bellos et al., 2018a]. The receiver can be trapezoidal or evacuated tube coupled to a secondary reflector and it is stable at a height of around 3 to 5 m over the ground [Moghimi et al., 2015]. This design presents a low cost, low mechanical difficulties compared to the PTC and so it is a promising choice for the future [Zhu et al., 2014; Morin et al., 2015]. But the optical efficiency of the LFR is relatively low due to the spaces between the primary mirrors, the shading and blocking effects in the primary mirrors, as well as the high ratio of the focal distance to the length (F/L) which increases the optical end losses. So, it is obvious that there is a need for increasing the optical efficiency of the LFR [Canavarro et al., 2016; Moghimi et al., 2017].

In this direction, there are some important literature studies which are focused on the calculation of the optical losses in LFR. In 2013, Zhu [2013] developed an analytical methodology for determining the optical losses of an LFR which was based on vector analysis. In 2014, Heimsath et al. [2014] developed a simplified model for the end losses prediction in the LFR and they calculated the optical performance of a collector using the factorization methodology. One year later, Hongh et al. [2015] developed a least square based method for the determination of the optical end losses in an LFR with 6% accuracy. Recently in 2018, Bellos and Tzivanidis [2018] suggested analytical equations for the determination of the incident angle modifiers of the LFR in the longitudinal and in the transversal directions.

Moreover, in the literature, there are many studies which have applied various ideas for improving the optical performance of LFR. The use of an azimuth tracking system has been studied by Huang et al. [2014] and it is found that the yearly thermal efficiency at 400^{o}C is 61% which is higher than the conventional LFR. The use of a compact LFR has been suggested by Zhu and Chen [2018] who developed a system with low land utilization and concentration ratio close to 15. Manikumar et al. [2014] studied a configuration of a short LFR with East-West tracking system. Zhu et al. [2017] investigated a scalable LFR system which moves in order to be vertical to the sun rays and in this configuration both mirrors and receivers are movable. In this

direction, Pulido-Iparraguirre et al. [2019] studied an elevated LFR with an inclined mirror field. In this design, the power production can be enhanced by up to 62%. Moreover, Ma and Chang [2018] found up to 50% thermal efficiency enhancement with this idea. The last part of the literature studies includes ideas about reducing the end loses without indication of the primary concentrators or East-West movement. Hongh and Larsen [2018] examined the extension of the receiver for some meters after the concentrator end. This idea can be beneficial, especially during the winter months. Furthermore, Yang et al. [2018] suggested the movement of the primary mirrors in the collector linear direction in order to reduce the end losses. They found that this idea is able to increase the performance by up to 50%.

Except for the LFR, there are many studies in the literature about the optical enhancement of PTC. Sun et al. (2017) examined the use of a double-axis PTC which can improve the performance up to 68.8% compared to the single-axis tracking system in the North-South direction. Moreover, Bellos and Tzivanidis (2019) examined the use of a booster reflector at the end of the PTC and they found yearly optical enhancement about 21.7%. Qu et al. (2017) studied a PTC solar field a rotating platform and they found about 5% daily performance enhancement compared to the single-axis PTC field. Lastly, it has to be said that Wang et al. (2017) performed an interesting work about the on-site optical and thermal measurement of a PTC solar field in order to be able to evaluate properly every system. More specifically, they developed and validated polynomial equations about the thermal losses of the receiver.

The previous literature review indicates that there is a lot of interest in finding ways for enhancing the optical efficiency, especially in the short LFRs. The present work investigates novel ideas in this regard. More specifically, three different ideas are studied numerically for an LFR with focal distance to length ratio (F/L) equal to 0.5. The first examined idea is the use of an extended receiver and it has similarities with by Hongh and Larsen [2018]. The second idea is a new one and includes the displacement of the receiver to avoid the non-illuminated receiver part at the beginning of the solar field. The third idea is the combination of the previous techniques which is also a proposed novel idea in the field of LFR. In every case, a parametric study is conducted in order to determine the optimum design. The collector performances are carried out for different solar angles. Moreover, the different configurations are evaluated on a yearly basis for the climate conditions of Athens (Greece) to calculate the real energy enhancement of each case. The analysis is conducted with a developed optical model in SolidWorks Flow Simulation software [SolidWorks, 2015].

2. Materials and Methods

2.1 The examined Linear Fresnel reflector

In this work, an LFR with flat primary mirrors and an evacuated tube receiver is investigated. This collector has been also studied in previous studies [Bellos and Tzivanidis 2018; Bellos et al., 2018b; Bellos et al., 2018c] and it is depicted in figure

1. The secondary concentrator is a compound parabolic concentrator (CPC) which has been optimized in work [Bellos et al., 2018b] using Bezier polynomial parameterization. Table 1 lists all the information about this collector. The maximum optical efficiency is 75.84% which is a relatively high value of an LFR. The initial length of the LFR module (L) is 6 m and the focal distance (F) is 3 m, while the total width (W) is also 6 m. The net aperture of the collector (A_a) is 27 m^2. The examined configuration has a relatively low length and it is suitable for applications with nominal power up to 25 kW such as solar cooling in buildings or for industrial processes. A characteristic parameter of this system, the focal distance to the length ratio is (F/L=0.5).

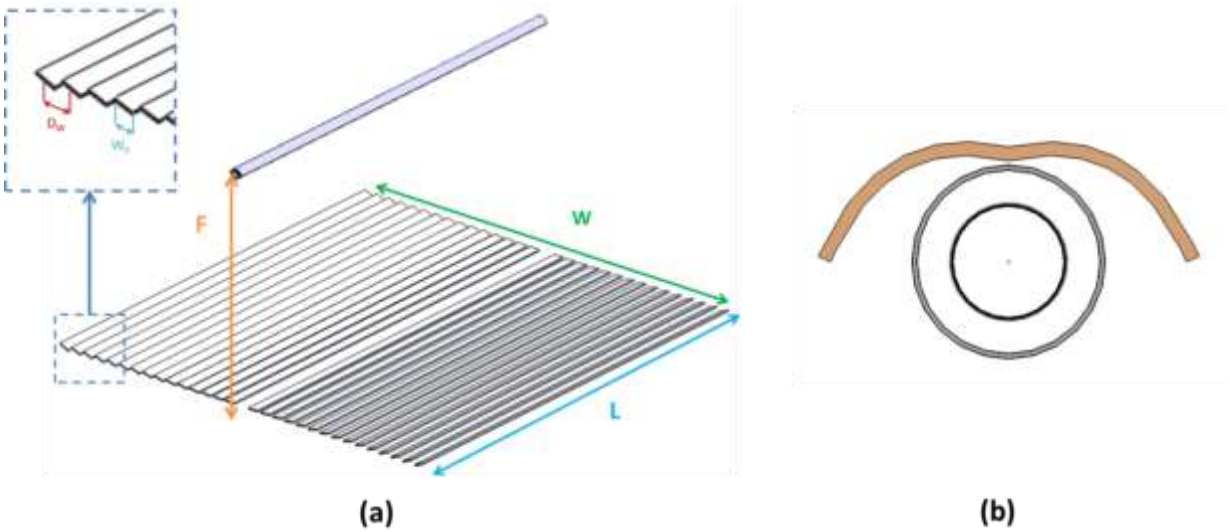

Figure 1. The examined initial configuration a) The total LFR b) The examined receiver with a CPC secondary reflector

Table 1. The basic parameters of the examined collector [Bellos et al., 2018b]

Parameter	Symbol	Value
Primary reflector field width	W	6 m
Primary reflector field length (nominal)	L	6 m
Primary parabola focal distance	F	3 m
Mirror width	W_0	0.15 m
Distance between mirrors	D_w	0.2 m
Number of the primary mirrors	N_{rf}	30
Net aperture of the concentrator	A_a	27.0 m^2
Concentration ratio	C	20.46
Absorber inner diameter	D_{ri}	0.066 m
Absorber outer diameter	D_{ro}	0.070 m
Cover inner diameter	D_{ci}	0.109 m
Cover outer diameter	D_{co}	0.115 m
Cover transmittance	τ	95%
Absorber absorbance	α	92%
Primary reflector reflectance	ρ_1	94%
Secondary reflector reflectance	ρ_2	94%
Secondary reflector efficiency	η_{sec}	97.5%
Maximum optical efficiency of the LFR	$\eta_{opt,max}$	72.84%

2.2 Problem description

The optical efficiency of the LFR is depended on the solar position and in particular, is determined by the projection of the solar incident angle (θ) on the longitudinal and transversal directions. The projected solar angles on transversal and longitudinal directions are respectively called transversal angle (θ_T) and longitudinal angle (θ_L).

The optical efficiency of a plant reduces when the solar angles increases. The incident angle modifier (IAM or K) is the standard terminology in the determination of the optical efficiency of linear CSP plants based on θ_L, θ_T. The IAM is defined as:

$$K(\theta_L, \theta_T) = \frac{\eta_{opt}(\theta_L, \theta_T)}{\eta_{opt}(\theta_L=0, \theta_T=0)} \quad (1)$$

Moreover, the IAM along the longitudinal (K_L) and transversal (K_T) directions are defined as:

$$K_L(\theta_L) = \frac{\eta_{opt}(\theta_L, \theta_T=0)}{\eta_{opt}(\theta_L=0, \theta_T=0)} \quad (2)$$

$$K_T(\theta_T) = \frac{\eta_{opt}(\theta_L=0, \theta_T)}{\eta_{opt}(\theta_L=0, \theta_T=0)} \quad (3)$$

The total IAM (K) is defined as the product of the other two IAMs [Gaul and Rabl, 1980]:

$$K(\theta_L, \theta_T) = K_L(\theta_L) \cdot K_T(\theta_T) \quad (4)$$

The objective of this work is to investigate some novel techniques for reducing the impact of the longitudinal IAM (K_L) on the short linear collector performance because this parameter is extremely important in the performance evaluation of short LFR as the present one. Also, it is a critical parameter which reduces drastically the performance of the LFR during the winter period. The theoretical value of the K_L for an LFR with North-South orientation has been suggested by Bellos and Tzivanidis [2018] is:

$$K_L(\theta_L) = \cos(\theta_L) - \frac{F}{L} \cdot \sqrt{1 + \left(\frac{w}{4 \cdot F}\right)^2} \cdot \sin(\theta_L) \quad (5)$$

This equation shows that the (K_L) takes into account the sun position due to the term "cos(θ_L)" and also it includes the optical end losses with the second term. Figure 2 depicts the end losses in the examined collector. Practically, there is a non-illuminated area at the beginning of a collector with a length of (L_{sh}) and this fact leads to a loss in optical performance of the plant. So, the absorbed solar irradiation in the absorber is getting lower when the longitudinal solar angle increases.

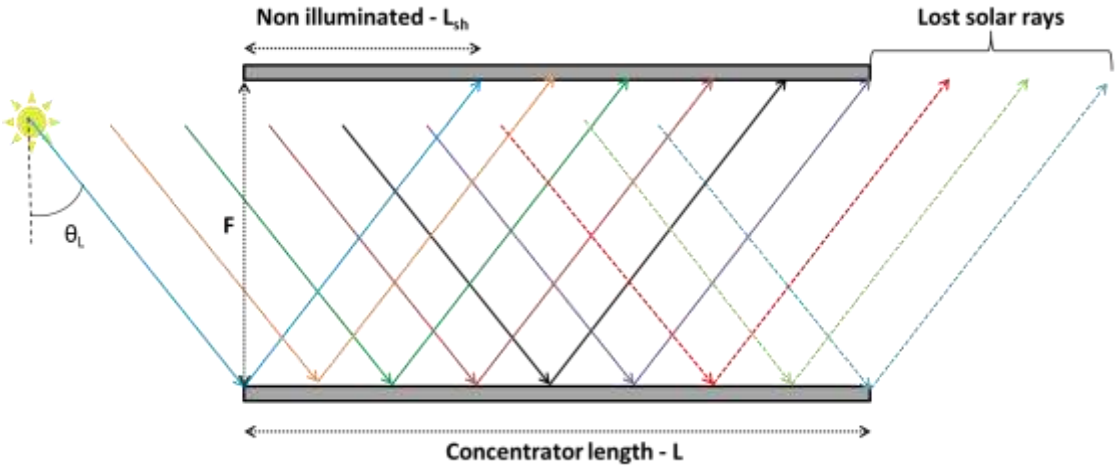

Figure 2. End losses in a linear Fresnel reflector

2.3 The examined ideas

In this work, three different cases are studied to enhance the optical efficiency of an LFR by reducing the end losses. It is assumed that the IAM in the transversal direction (K_T) is constant among the examined cases because the relative positions of the primary mirrors do not change and hence the shading and blocking effects are the same as the initial case. Moreover, this work assumes that the cosine effect, which is very important in the great transversal angles, is assumed to be the same among the examined cases.

2.3.1 Increase of the receiver length

The first examined idea is an increase in the receiver length after the concentrator end and this idea is illustrated in Fig. 3. In practice in the northern hemisphere, such an increase should be placed along the north direction since the solar rays come from the equator (the south of the plant). The length increase is achieved by adding an extra receiver part with a length of L_{ext}. The analysis is performed using the dimensionless parameter (λ) or length ratio which is:

$$\lambda = \frac{L+L_{ext}}{L} \tag{6}$$

This parameter takes values from 1.0 to 2.0 in this scenario. Higher values lead to extremely long receiver configurations and practically there is no sensible gain beyond λ=2.0. Figure 3 shows that the extra receiver length leads to lower loss of reflected rays beyond where the collector ends and so the optical efficiency and the K_L of the plant are enhanced. It is important to note that this technique has increased both the capital cost and thermal losses of the system due to implementing the longer receiver (both evacuated tube and secondary concentrator) to enhance the optical efficiency.

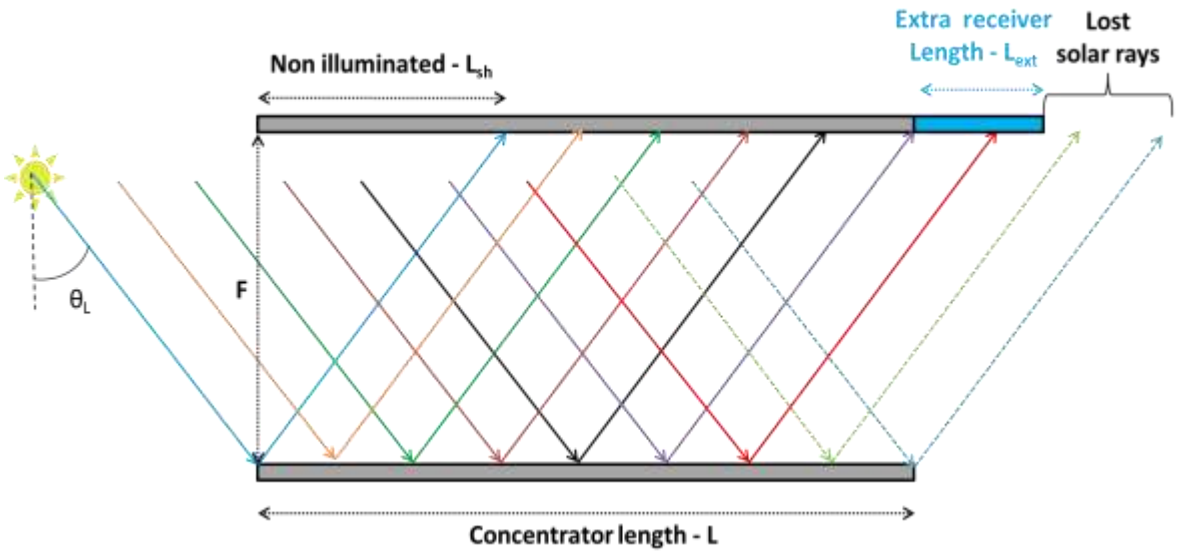

Figure 3. Enhancing the optical efficiency by extending the receiver along the longitudinal north direction (cases with λ > 1.0)

2.3.2 Receiver displacement

Usually, the small incident angles rarely take place in real operational condition due to the solar movement during the day and the different position during the year. More specifically, the solar angle is higher in winter and lower in the summer period. Moreover, for example, in locations with geographical latitude above 25^o, the solar angle is rarely small (in the range of 5^o to 10^o) and so there are significant optical losses due to the sun altitude. Therefore, the non-illuminating effect at the start of the receiver can't be neglected. This fact pops up the idea of displacing the receiver longitudinally to exploit the impinging solar rays at the end of the concentrator and minimize the non-illuminated region. This technique could be very beneficial in high solar angles but less effective in low solar angles, in comparison with the conventional design. Figure 4 illustrates this examined idea which presents lower lost rays at the end and smaller non-illuminated region in a typical case.

The analysis of this scenario is conducted using the dimensionless parameter (dx) which is the displacement parameter and is defined as the displacement distance (P) to the concentrator length (L):

$$dx = \frac{P}{L} \tag{7}$$

The parameter dx is studied from 0.0 up to 1.0 in order to cover all the possible relative positions between concentrator and receiver. Higher values of the dx would lead to zero performance in small incident angles which is not desirable. Moreover, it is important to state that this technique does not impose a great extra cost to the design and also the receiver thermal loss would not increase since the same receiver length as proposed in the conventional design is used. The cost of the system can increase due to the modified supporting structure system.

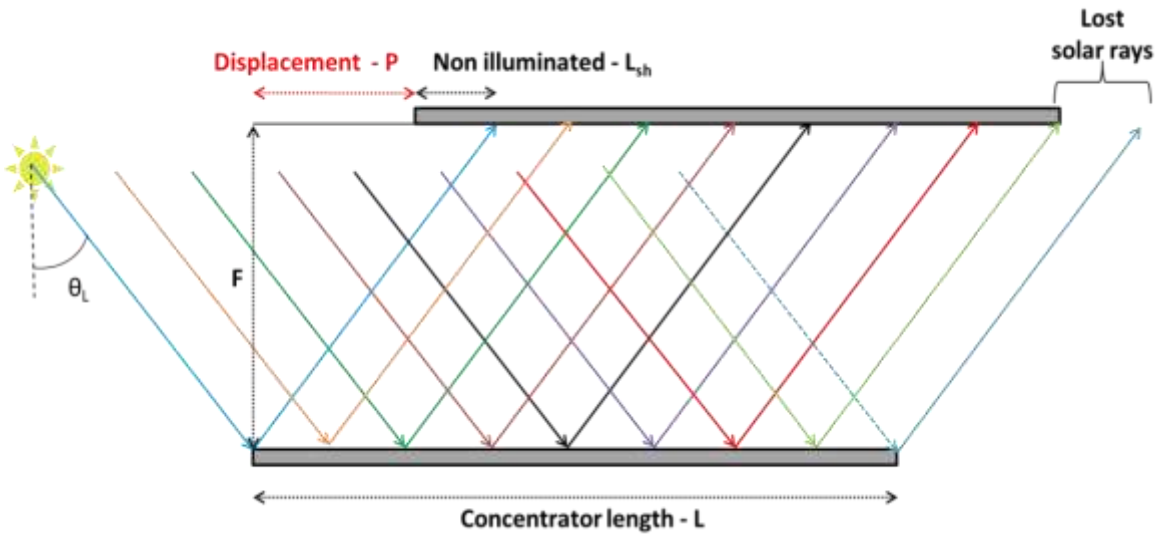

Figure 4. Enhancing the optical efficiency by shifting the receiver along the longitudinal direction (cases with dx > 0.0)

2.3.3 Hybrid scenario (combination of the two techniques)

The last examined idea is the combination of the previous techniques in order to enhance the optical performance of the LFR. This case has an interest because utilizing a small displacement will reduce the need for a very long receiver and therefore, the cost increase would be reasonable compared to the idea of section 2.3.1. At this point, it would be important to state that the increase of the investment cost is estimated to be up to 10% of the total LFR cost. The extra cost regards the greater evacuated tube length, as well as the extra supporting system for this part. However, the exact estimation of the increased cost is not possible due to the great variety of the designs and of the different module lengths that exist in the commercial LFR.

So, in this analysis, the parameter dx is studied up to 0.5, while the parameter λ up to 1.8. The final results proved that the examined ranges are generous enough to determine the optimum design in every case which maximizes the optical performance of the collector. Figure 5 shows the examined idea of the hybrid design which leads to a lower non-illuminated area at the beginning of the receiver and to lower loss of solar rays at the end.

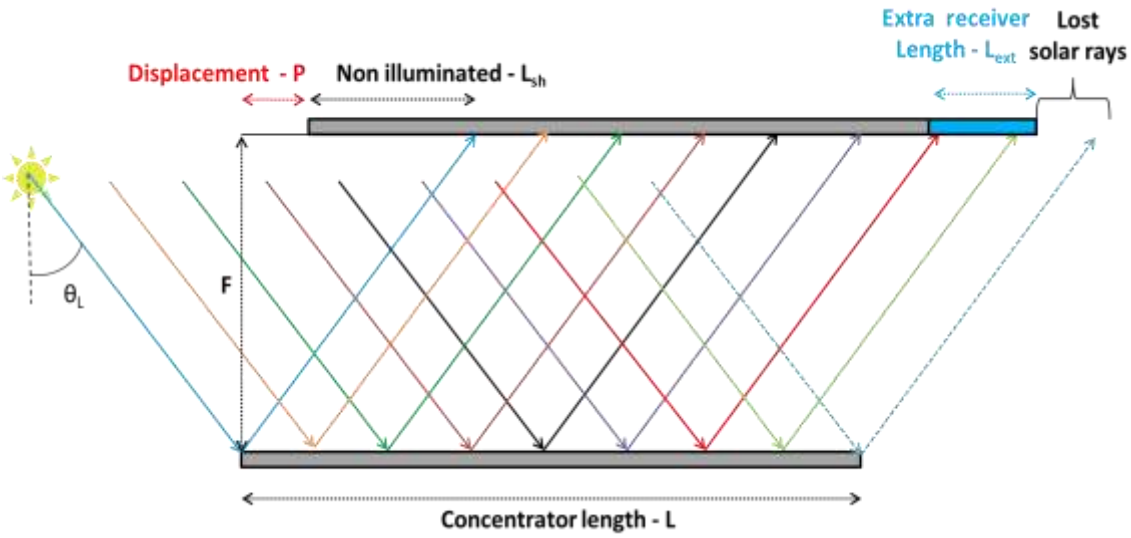

Figure 5. Enhancing the optical efficiency by extending and shifting the receiver along the longitudinal direction - hybrid design (cases with λ > 1.0 and dx > 0.0)

2.3.4 Methodology for the calculation of the longitudinal IAM

The optical analysis is conducted with a developed model in SolidWorks Flow Simulation Studio [SolidWorks, 2015]. This program has been used in numerous studies about solar systems and more specifically in our previous studies [Bellos et al. 2016, Bellos et al. 2018a, 2018b, 2018c, 2018d] so it can be assumed as valid. More specifically, it has to be said that in the study of Bellos et al. (2016) there is the validation of an LFR model with experimental results, something that makes the followed methodology to be stronger. For every scenario, as the solar position changes, the (K_L) is calculated. The solar angle (θ_L) is studied from 0^o up to 90^o with a step of 5^o in order to cover all the possible operating conditions. The examined scenarios are summarized in table 2. It is also useful to state that totally 10^7 solar rays are used in order to have converged results and this number is determined with a simple sensitivity analysis.

Table 2. The variable values in the examined cases

Cases	$\lambda=(L+L_{ex})/L$	dx=P/L
Initial design	1.0	0.0
Increase of the receiver length	1.0 to 2.0 (with 0.1 step)	0.0
Receiver displacement	1.0	0.0 to 1.0 (with 0.1 step)
Hybrid scenario (combination)	1.0 to 1.8 (with 0.2 step)	0.0 to 0.5 (with 0.1 step)

2.5 Yearly performance evaluation

The final step in this work is the yearly evaluation of the different examined scenarios. Using the IAM in the longitudinal direction in every case and the weather data for Athens, Greece (37° 59'N, 23° 43'E), the yearly enhancement in the optical efficiency is calculated. The yearly weather data have been presented in the studies of Bellos et al. [2017, 2018c] and Kouremenos et al. [1985]. For the sake of brevity, these weather data are excluded in this paper. It is noteworthy that only the sunny

days of every month in Athens are taken into consideration as in the study [Bellos and Tzivanidis, 2019].

A critical assumption of this work is that the variation of the IAM in the transversal direction is the same for all the different examined LFR designs. The relative positions between the mirrors are the same among the examined cases and so the blocking and the shading effects are not affected by the receiver design. So, by using the data in the study of Bellos and Tzivanidis [2018] about the IAM in the transversal direction of the initial (conventional) design, then the IAM in the transversal direction of all the designs is known.

The mean yearly IAM (K_m) is calculated as:

$$K_m = \frac{\sum_{i=1}^{12} SN_{day,i} \cdot \int_{t=0}^{t=N_i} K_L \cdot K_T \cdot G_b \cdot dt}{\sum_{i=1}^{12} SN \cdot \int_{t=0}^{t=N} G_b \cdot dt} \quad (8)$$

The counter (i) regards the months of the year, the parameter ($SN_{day,i}$) the sunny days of every month and the (N_i) is the day duration of the monthly mean day. By taking into consideration only the sunny days, the LFR is properly evaluated because the cloudy days its operation faces important difficulties. Practically, the mean IAM takes into account the energy production for the different solar incident angles and it is a proper index for the evaluation of every design. This parameter is directly associated with the useful heat production of the LFR and thus the maximization of this parameter is the goal of this study.

3. Results and discussion

3.1 Increase of the receiver length

The first examined idea is the use of an extended receiver with length ratio (λ) up to 2. The IAM in the longitudinal direction (K_L) is depicted in figure 6 for different receiver lengths and incident angles (θ_L). This figure clearly shows that the higher length of the receiver would enhance the IAM for all the incident angles. This is a reasonable result due to the end losses reduction with the extended receiver. It can be said that the receiver extension up to +50% leads to significant optical performance improvement, while the improvement after this limit would be insignificant. Another useful conclusion from this figure is that the receiver length increase makes the IAM curve to be very close to the cosine curve for the small incident angles. For instance, the curve of λ=1.1 is close to the cosine curve up to 10^o, the curve of λ=1.2 up to 20^o while the curve of λ=1.5 up to 35^o. The cosine curve is practically the upper limit for all the cases (proved in figure 6, as well) because the LFR can exploit the solar irradiation in a horizontal plane which is created by the primary mirrors [Bellos et al., 2018e].

However, the performance enhancement is different for the various incident angles. So, the yearly performance of every design is evaluated for the location of Athens

(Greece) in figure 7. Figure 7 clearly indicates that the yearly performance is enhanced with the longer receiver length. The initial design has yearly mean IAM equal to 37.2%, while the case with λ=2.0 has 55.9% which means 50.3% enhancement. This is a significant increase but it is associated with a great receiver increase. The case of λ=1.5 leads to 52.3% mean IAM which means 40.6% enhancement. So, it can be said that after a limit, which is around λ=1.5, the receiver length increase leads to small further enhancements and so it is not so cost effective.

Moreover, it has to be said that the longer receiver is beneficial for all the months but especially for the winter months where there are greater solar angles. During the winter months, the length increase leads to significant enhancement of the IAM. For the summer months, a 30% extension of the length is able to maximize the collector performance, while for months as to October a length extension of 70% is the optimal one for IAM maximization.

As a final conclusion of the first examined idea, it can be said that a receiver extension between 30% and 50% is really beneficial because it leads to significant optical improvement throughout a year and it will maximize the IAM during the summer period where the LFR usually operate. On the other hand, if the LFR is used in a winter application, the receiver length can be extended more. However, in any case, the cost increase and thermal losses have to be taken into consideration.

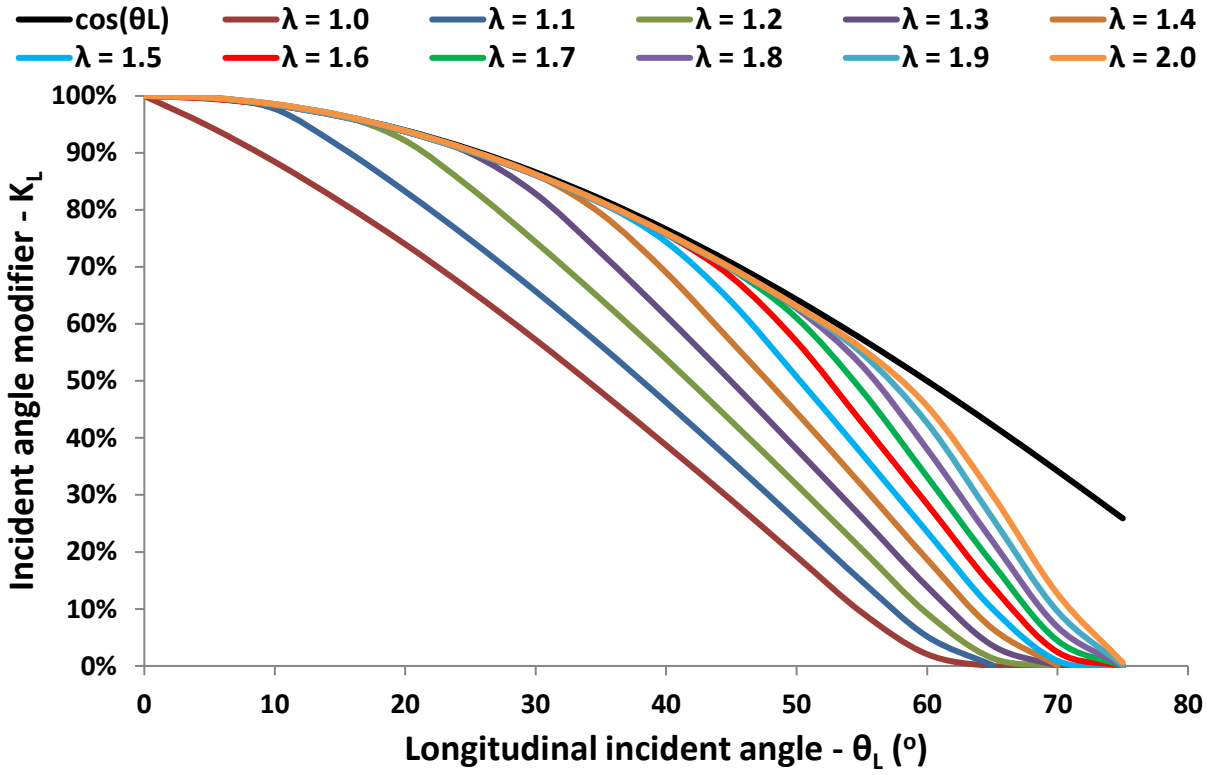

Figure 6. IAM for different solar angles for the case of extended receiver (dx = 0.0)

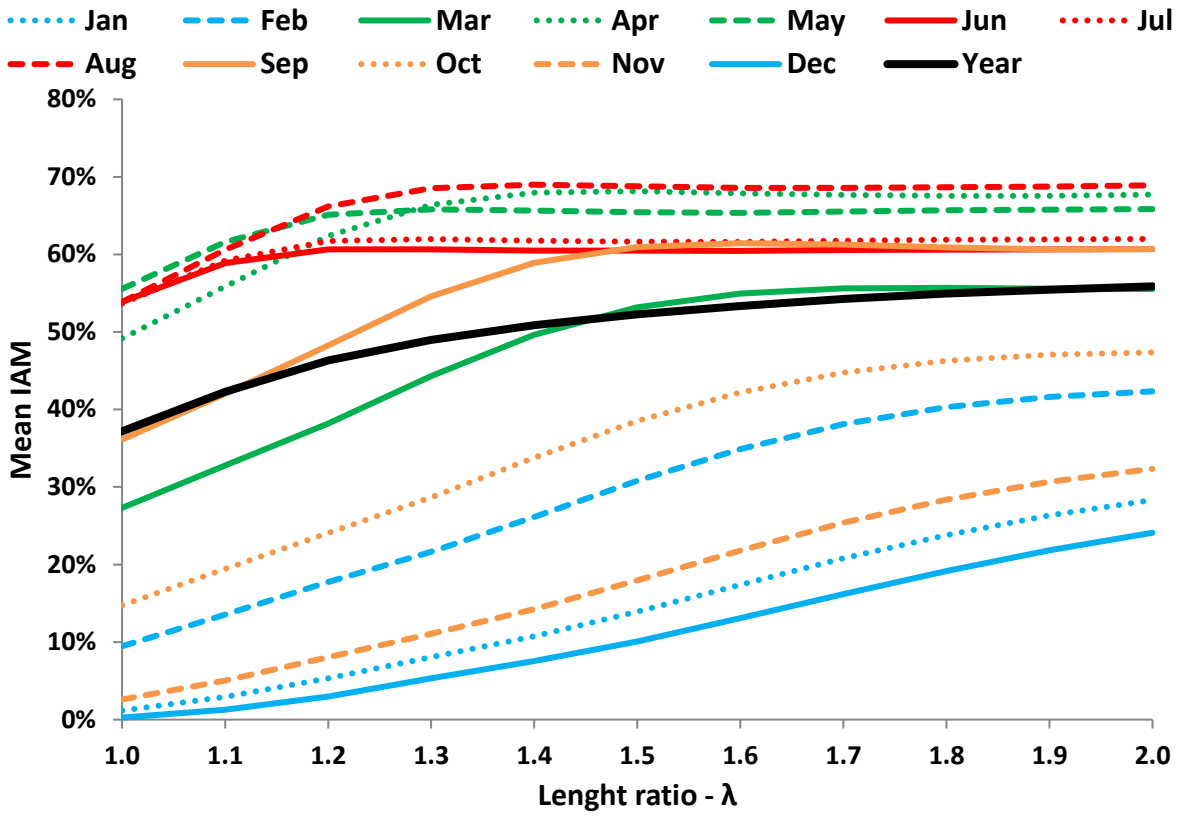

Figure 7. Monthly and yearly mean IAM for the cases of the extended receiver (dx = 0.0)

3.2 Displacement of the receiver

The second examined idea is the implementation of a displaced receiver with despoilment ratio (dx) up to 1. The IAM in the longitudinal direction (K_L) is illustrated in figure 8 for different receiver displacements and incident angles (θ_L). It is noteworthy that the IAM curves have a different shape than the conventional curves and they present an optimum value for a specific incident angle. For instance, the curve of dx=0.1 starts from K_L=94.92% for θ_L=0^o and has an increasing rate up to θ_L=10^o where the K_L is maximized at 97.64%. For higher incident angles, the K_L has a decreasing rate and a similar trend with the curve of the conventional design (dx=0.0). This trend is found for the entire displaced receivers but higher displacements lead to higher optimum indigent angles. More specifically, for dx=0.2, 0.3 and 1.0 the incident angles which maximize the IAM respectively take place at 20^o, 30^o and 60^o. In practice, the displacement utilization creates lower and higher performances at smaller and greater incident angles, respectively. This is the reason for the existence of an optimum point in every curve. At the optimum case, all the solar rays which reflected from the primary concentrator are approximately delivered to the receiver and in this case, the IAM is close to the cosine value. The cases with higher displacement are more efficient in higher incident angles and they are less efficient in low incident angles.

The yearly evaluation of these cases is presented in figure 9. There is an optimum displacement at dx=0.2 which maximizes the IAM to 44.7%. This scenario presents a

20.2% enhancement compared to the initial case. This enhancement is lower than the enhancements of section 3.1 about the extended receiver idea, but in the present case of the displaced receiver, there is not an important capital cost increase which is a great advantage of this technique. Only a cost increase due to the modified supporting structure is needed, while the receiver length is the same as the conventional design. As displayed, the optimum displacement for the summer months is about dx=0.2 to 0.3, while for winter months the optimum displacement is in the ranges of dx=0.8 to 1.1. The yearly optimum range for the dx is about 0.2 to 0.3 and follows the summer curves behavior because in this period there is greater solar energy potential.

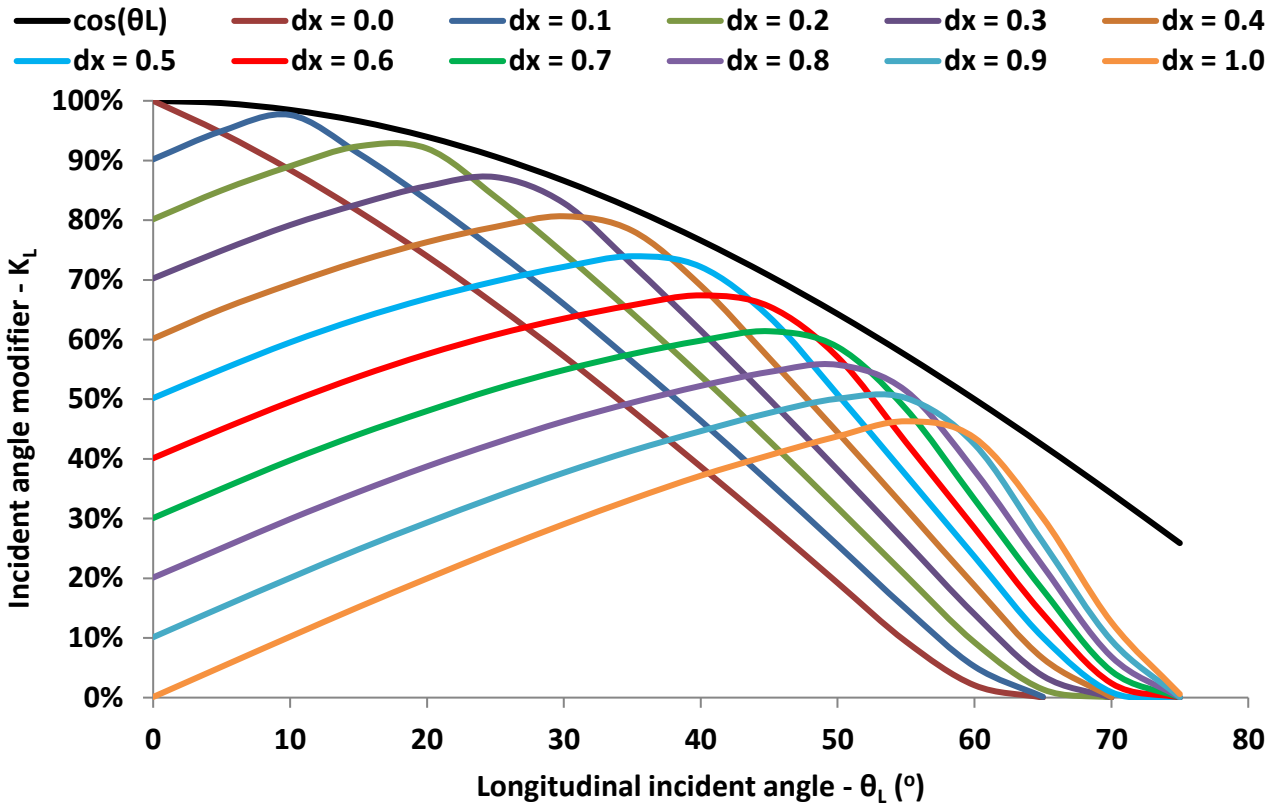

Figure 8. IAM for different solar angles for the case of the displaced receiver (λ = 1.0)

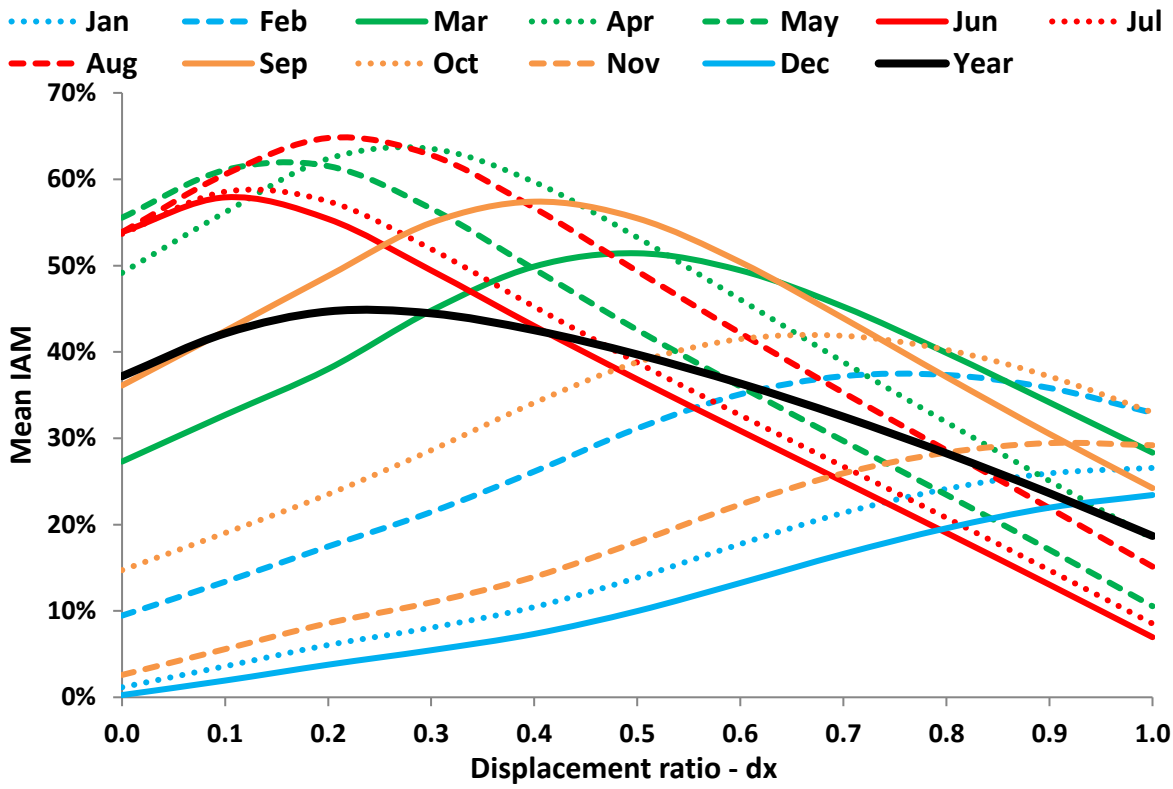

Figure 9. Monthly and yearly mean IAM for the case of the displaced receiver (λ = 1.0)

3.3 Hybrid design

Sections 3.1 and 3.2 have proved that the utilization of both the receiver extension and displacement techniques are beneficial for improving the mean IAM of the LFR. However, the cost increase with the receiver extension is a limitation and so the combination of the two examined techniques is proposed as a third method (the hybrid method). The goal of this method is to achieve high enhancements with a lower increase in the receiver length.

3.3.1 Incident angle modifier of the hybrid designs

In this section, the IAM curves for various hybrid designs are presented. As discussed, the hybrid design is created by the combination of the displacement receiver curve (in the first part) and the extended receiver curves (in the second part). Figure 10 depicts an example which verifies the previous statement. The red bullets correspond to a hybrid case of λ=1.2 – dx=0.2 and these points are on the displacement curve for λ=1.0 – dx=0.2 up to 15^o and comply with the extended curve for λ=1.4 – dx=0.0 beyond that point. Therefore, for solar angles greater than 15^o, the displaced receiver of λ=1.2 has the same performance of the receiver of λ=1.4 hence this option is a more cost-effective choice. However, there is an optical loss for solar angles lower than 15° which is the drawback of the hybrid design.

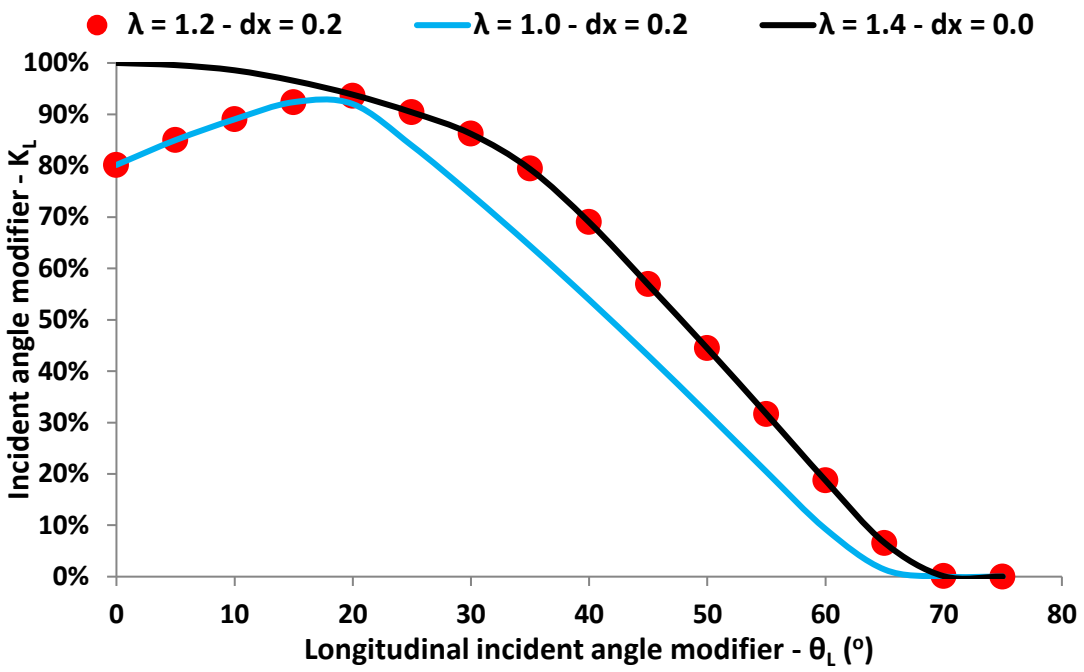

Figure 10. An example in support of the hybrid case as a combination of a case with the extended receiver and a case with a displaced receiver

The next step is the presentation of typical hybrid design IAM curves in figures 11 and 12 show the hybrid design IAMs for different displacements ratios up to 0.5. Figure 11 illustrates the designs with a length ratio equal to 1.4 and figure 12 with length ratio equal to 1.8. The results show that these designs have an initial part where the IAM has an increasing rate, then there is a part where the IAM is very close to the cosine line and eventually a third part where the IAM decreasing with a higher rate than the cosine shape. Practically, the hybrid curves are combinations of designs with displacement absorber (first part of the hybrid curve) and extended absorber (second and third part of the hybrid curve). Greater values of the parameter (λ) make the hybrid curves to have higher part close to the cosine curve.

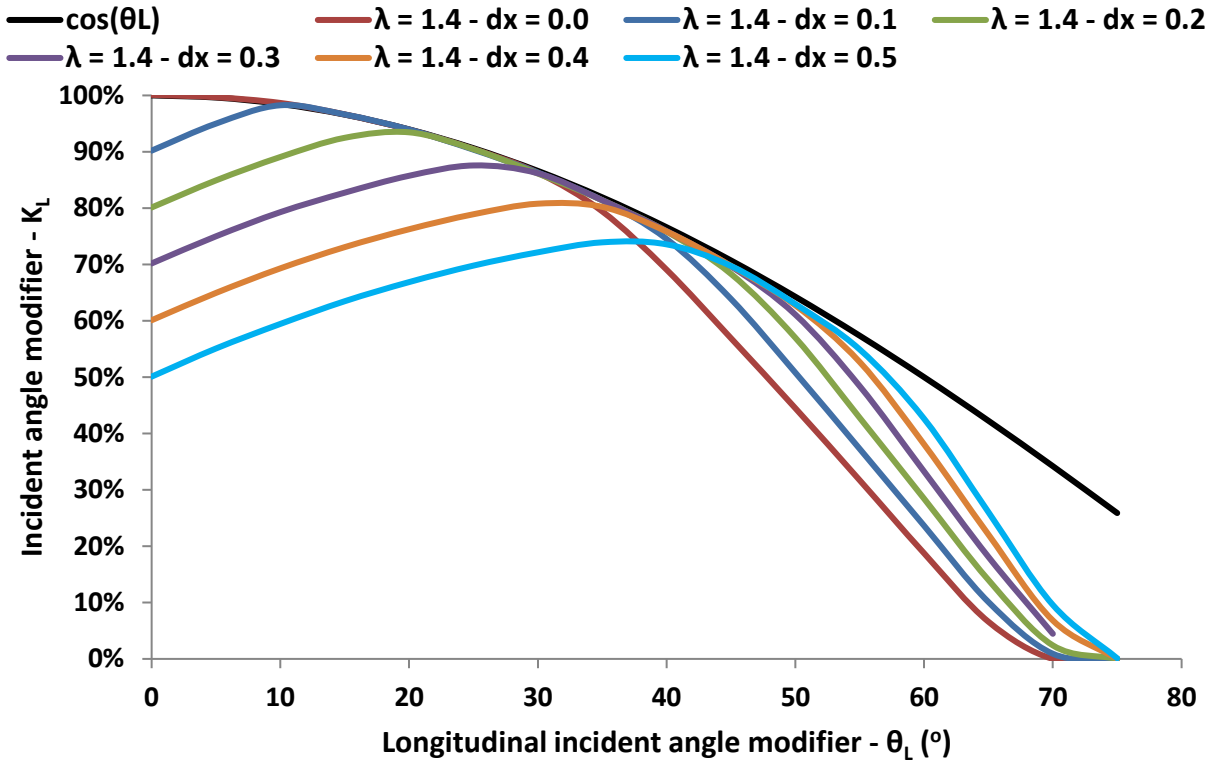

Figure 11. IAM for different solar angles for the hybrid cases with λ = 1.4

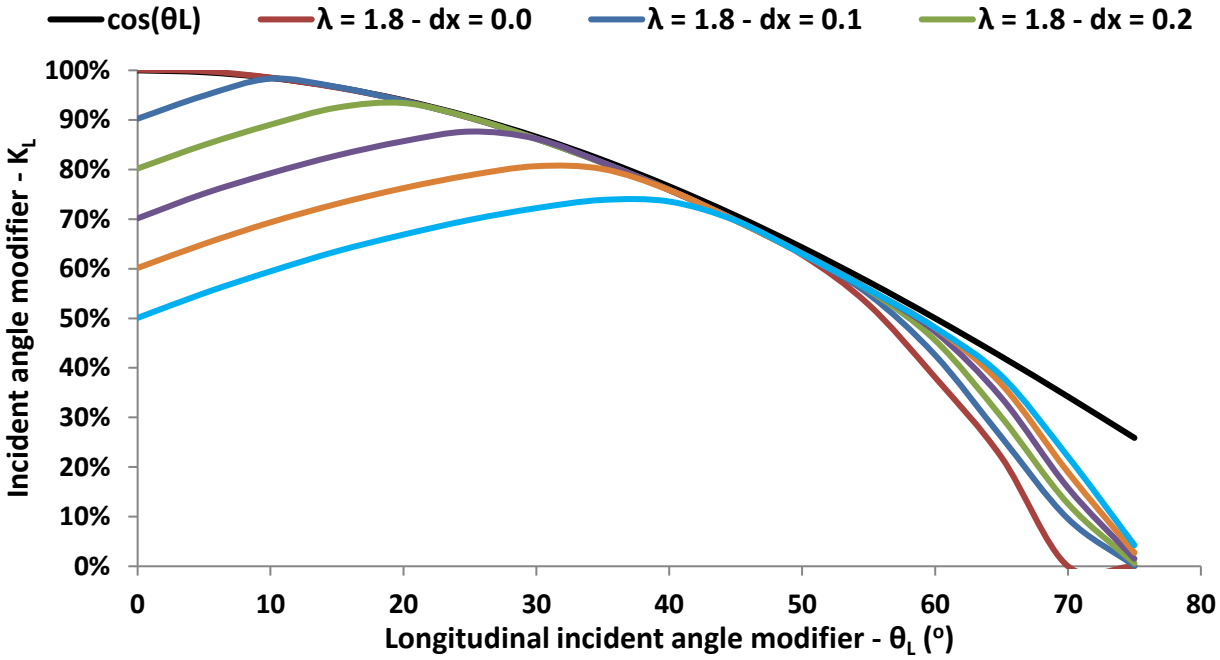

Figure 12. IAM for different solar angles for the hybrid cases with λ = 1.8

A next comparison is given in figure 13 where the curves of the extended receiver are compared against the hybrid cases with dx=0.1. It is obvious that all these hybrid curves have lower performance for incident angle up to 10^{o} and beyond this point, every hybrid curve is more efficient than the respectively extended curve with the same value of (λ).

Other useful comparisons are displayed in figure 14 about hybrid designs. These figures prove that the hybrid curves tend to follow the trend of the extended designs in great incident angles. Figure 13 shows that displacement implementation can reduce the need for an extended design. For example, the use of a receiver with λ=1.0 – dx=0.2 leads to the same performance of a receiver with λ=1.2 – dx=0.0 for incident angles after 20°. Indeed, the displacement utilization (dx) makes a hybrid receiver with a length ratio of λ to have the same performance as the extended design with a length ratio of λ+dx has beyond a critical incident angle. This result practically shows that the displacement is able to reduce the receiver cost length and lead to a cost-effective choice.

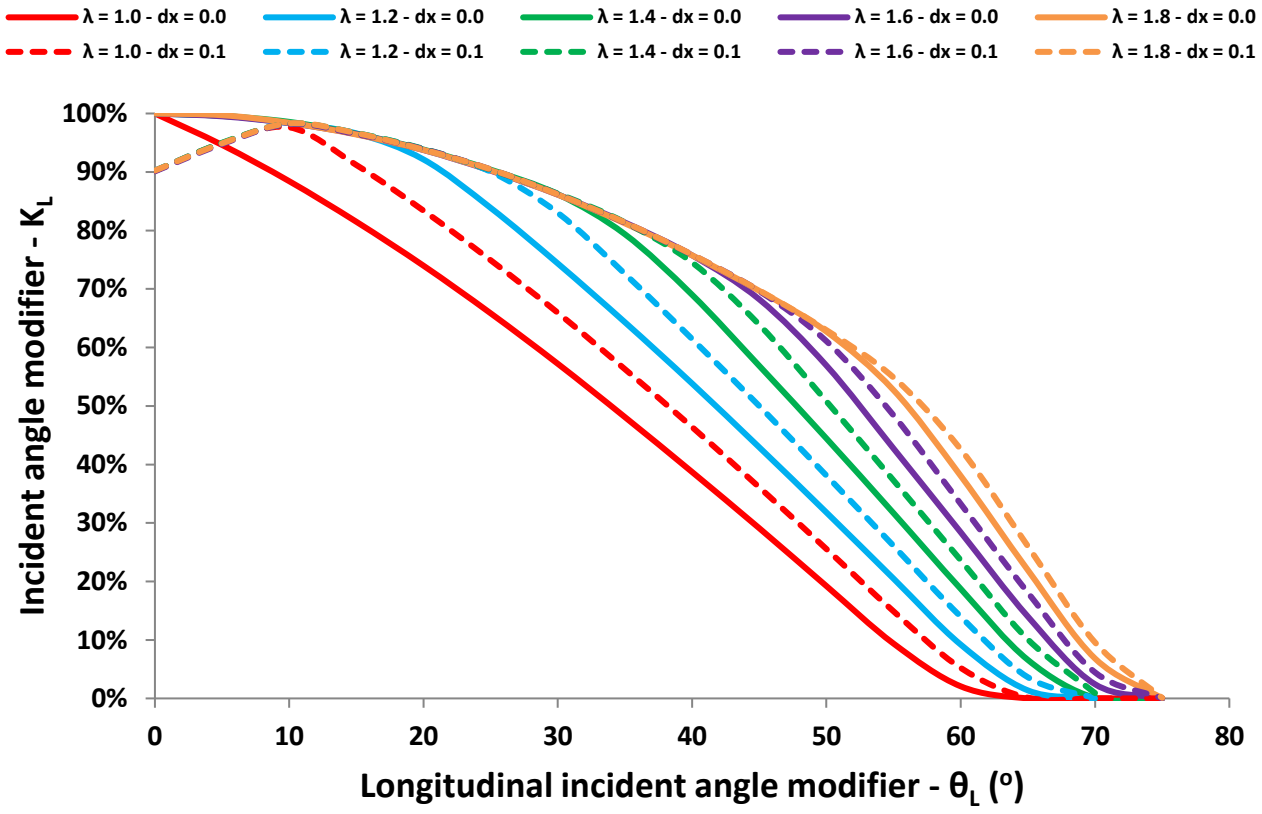

Figure 13. IAM for different solar angles for the cases with dx = 0.0 and dx = 0.1

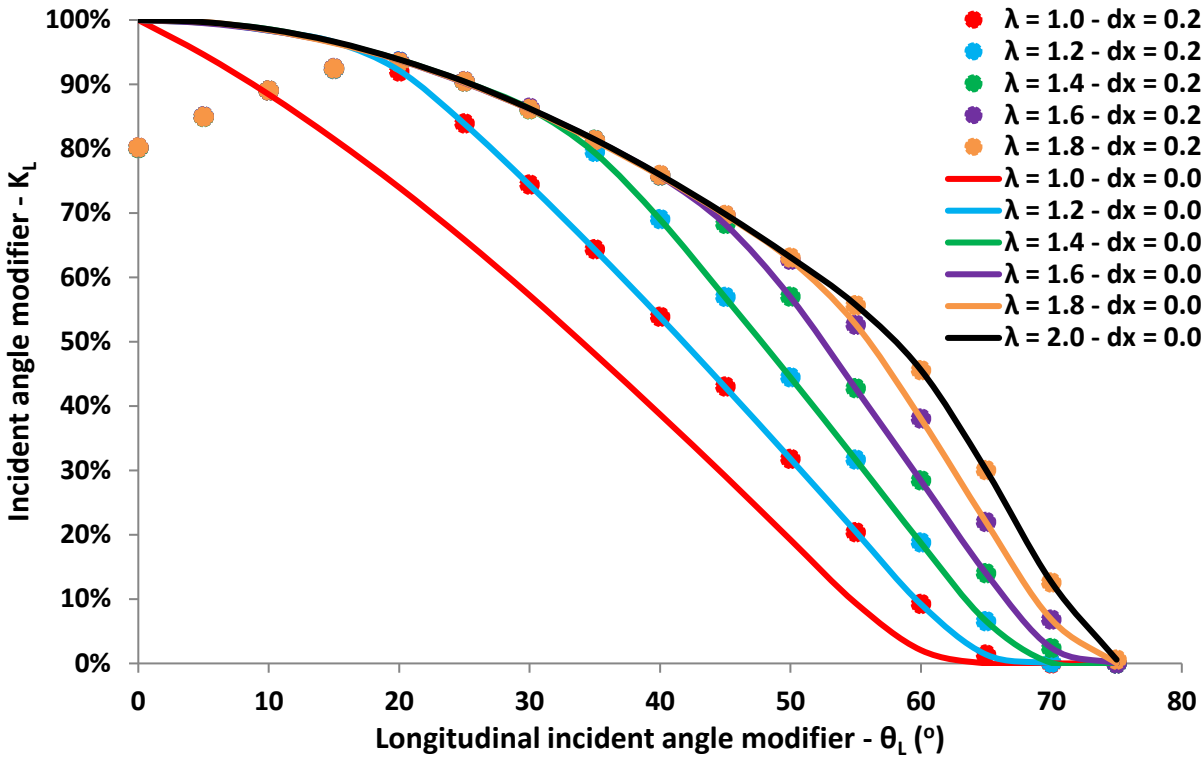

Figure 14. Comparison of IAM between extended cases and hybrid cases with λ = 1.2

3.3.2 Yearly and monthly performance of the hybrid designs

The next step is the investigation of the yearly performance of the hybrid designs for the climate conditions of Athens. Figure 15 shows the yearly performance for the various examined scenarios with λ=1.0 up to 1.8 with step 0.2, as well as dx=0.0 up to 0.5 with step 0.1. As displayed, the higher length parameter (λ) leads to higher mean yearly IAM. On the other hand, there is an optimum (dx) for each individual curve which maximizes the mean yearly IAM. For the case of λ=1.8, the maximum IAM is 55.3% at dx=0.1. While for the curves of λ=1.6 and λ=1.4, the optimum dx is 0.2 and the maximum IAM is 53.9% and 52.0% respectively. For the cases with λ=1.2 and λ=1.0, the maximum IAM is 49.2% and 44.7% respectively for dx=0.3. Table 3 summarizes the mean yearly IAMs for all the cases and table 4 shows the enhancement of every case compared to the initial design (λ=1.0 – dx=0.0). Table 3 shows that the maximum yearly IAM is 55.3% for the case (λ=1.8 – dx=0.2) and in this case, the enhancement is 48.7% according to table 4. For the cases with λ=1.0, the IAM is maximized for dx=0.2 and takes the value 44.7%, while for the cases with λ=1.4 the maximum IAM is 52.0% for dx=0.1. So, it is obvious that the optimum (dx) values are different for the different (λ) values.

Furthermore, figures 16 to 18 display the mean monthly results for June, September and December which are three characteristic months. Figure 16 shows that the curves are close to each other and this is attributed to the small incident angle in this month. Therefore, a small length extension is adequate for this month. As shown, the optimum displacement is about 0.2 for the λ=1.0, while it is zero for the other cases. Figure 17 indicates that the displacement of around 0.3 is optimum for September and

the curves of λ=1.4, λ=1.6 and λ=1.8 are close to each other. Lastly, figure 18 proves that higher displacement and higher length of the receiver are both beneficial in December.

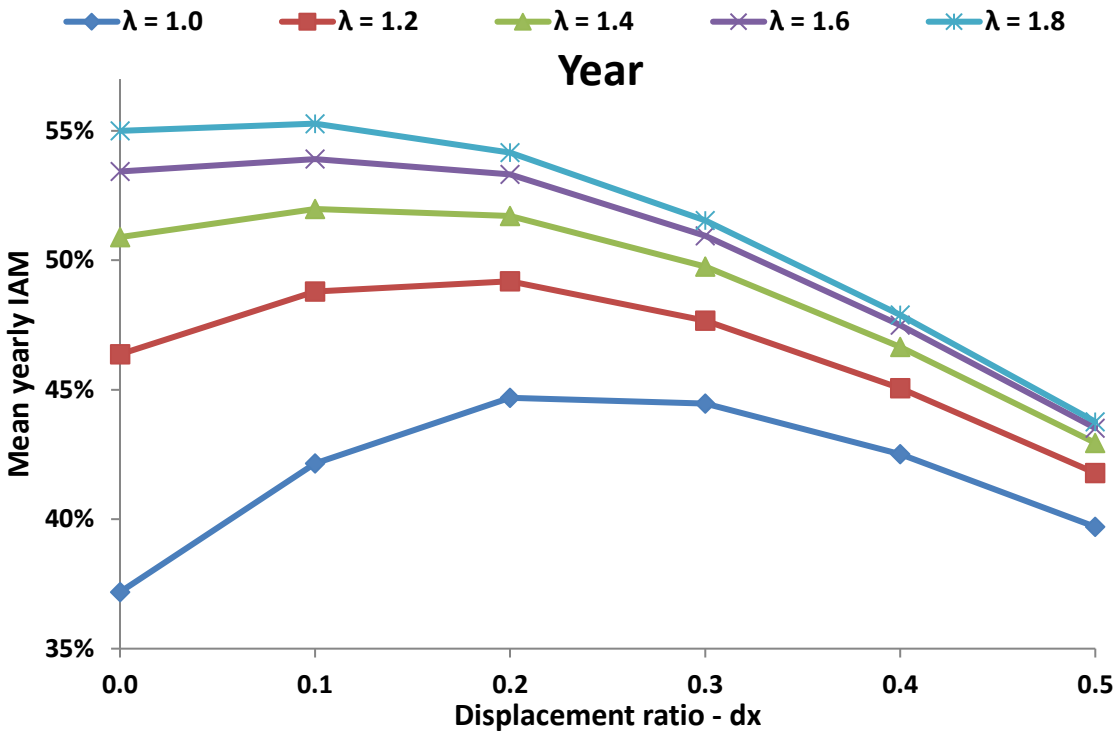

Figure 15. Mean yearly IAM for the various examined cases

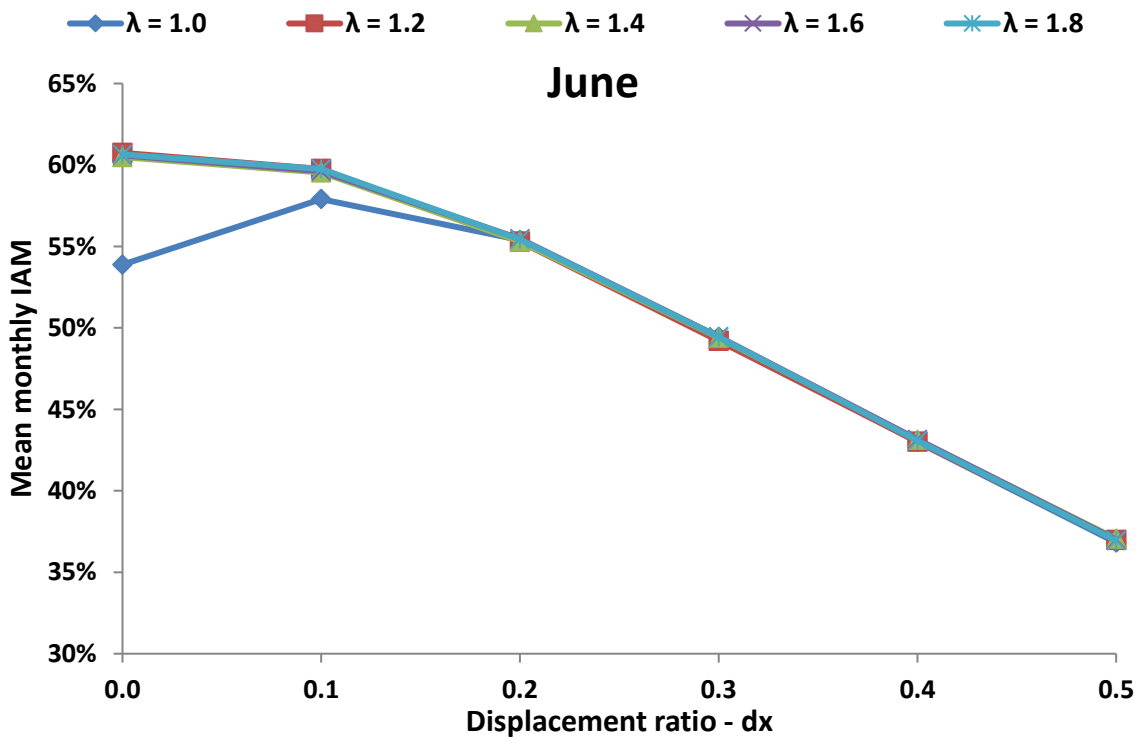

Figure 16. Mean monthly IAM in June for the various examined cases

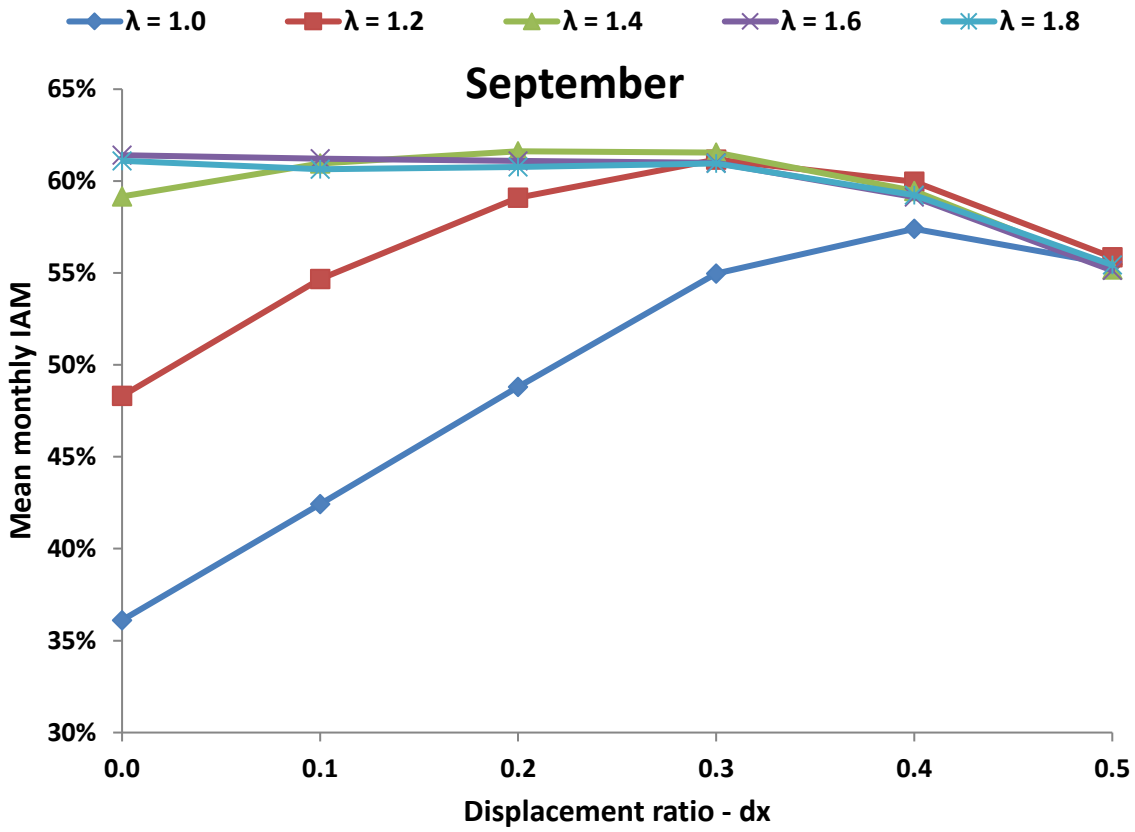

Figure 17. Mean monthly IAM in September for the various examined cases

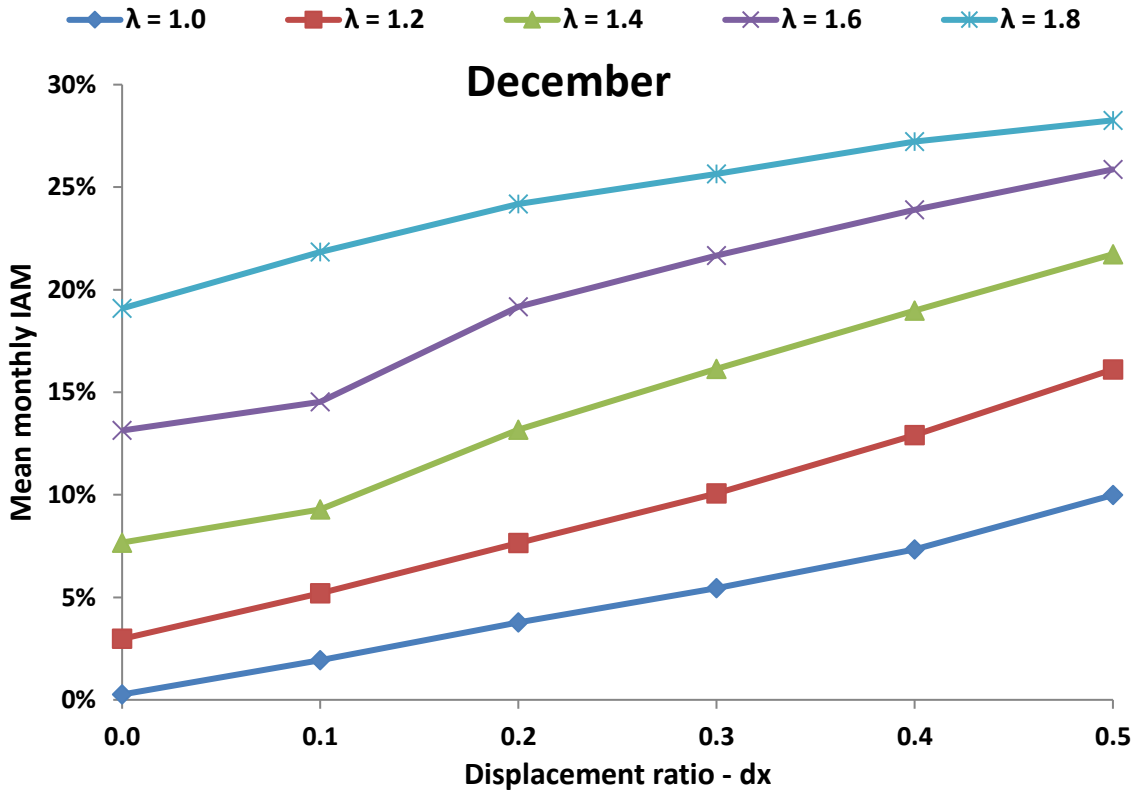

Figure 18. Mean monthly IAM in December for the various examined cases

Table 3. Yearly mean IAM for the different hybrid scenarios

dx	λ				
	1.0	**1.2**	**1.4**	**1.6**	**1.8**
0.0	37.2%	46.4%	50.9%	53.4%	55.0%
0.1	42.2%	48.8%	52.0%	53.9%	55.3%
0.2	44.7%	49.2%	51.7%	53.3%	54.2%
0.3	44.5%	47.7%	49.8%	51.0%	51.5%
0.4	42.5%	45.1%	46.7%	47.5%	47.9%
0.5	39.7%	41.8%	43.0%	43.5%	43.8%

Table 4. Yearly mean IAM enhancements for the different hybrid scenarios

dx	λ				
	1.0	**1.2**	**1.4**	**1.6**	**1.8**
0.0	0.0%	24.7%	36.9%	43.7%	47.9%
0.1	13.4%	31.2%	39.8%	45.0%	48.7%
0.2	20.2%	32.3%	39.1%	43.4%	45.7%
0.3	19.6%	28.2%	33.8%	37.0%	38.6%
0.4	14.3%	21.2%	25.5%	27.7%	28.8%
0.5	6.8%	12.4%	15.5%	17.0%	17.7%

At this point, it has to be said that the found enhancement are around up to 50.3% with the tube extension and up to 48.7%. These values are similar values with the reported enhancements by Yang et al. [2018] who found that the primary field movement can reach up to 50% enhancement. About the cost of the examined idea, the use of an extended receiver leads to a significant cost increase due to the extra receiver and the modified supporting system. However, the use of a displaced receiver has a small cost increase only due to the modified supporting system. The hybrid scenario is associated with an intermediate cost increase among the other ideas. So, for the proper selection of the examined ideas, a financial investigation has to be done in future studies. Generally, it can be said that the cost increase will not be high in all the cases and it is estimated up to 10% because it does not include any change in the primary mirror field. For short LFR which are located in locations with latitude over 25^o-30^o, the use of a displaced receiver seems to be a reliable choice due to the significant IAM enhancements and the small capital cost increase. Moreover, it has to be stated that the use of the suggested ideas can be easily done in the LFR plants because they are based on the extension or displacement of the existing geometry. More specifically, the extension of the receiver can be easily achieved by connecting and extra part of the evacuated tube in the North direction of the collector

4. Conclusions

The objective of the present work is the optical investigation of some novel ideas about the optical enhancement of the linear Fresnel reflectors. The reduction of the optical end losses is studied by using three techniques. The receiver length extension, the receiver displacement and the combination of the previous ideas (hybrid design) are the studied ideas in this work. The results are given using the incident angle

modifier (IAM) curves, as well as by calculating the yearly optical performance of the LFR in the location of Athens (Greece). The most important conclusions of this work are summarized below:

- The use of an extended receiver is able to increase the mean yearly performance up to 50.3% if a receiver with a double length is used. However, the use of a receiver with 50% longer length leads to 40.6%.

- About 20% receiver displacement of the collector length is able to enhance the yearly performance of the system by about 20.2%. This idea has not extra investment cost and it is financially viable in any case.

- The hybrid design is able to enhance the optical performance up to 48.7% and generally, it gives similar enhancement to the extended designs but with a lower receiver length. Practically the hybrid design is able to give a less expensive configuration than the simple extended receiver idea and with a similar optical enhancement.

-For each individual case, a proper optimization for the examined location requires, as well as a cost analysis in order to determine the optimum receiver design which can lead to the most viable investment.

- The proposed idea is crucial especially for the short LFRs and it has to be considered in future configurations. For longer LFRs, the enhancement always exists but they would be much lower. This fact can be studied in future studies. Moreover, future work is needed for investigating the examined idea in locations with different latitude. Another important point of the future studies can be the thermal analysis of the suggested LFR designs and the comparison with the conventional one.

Acknowledgments
Dr. Evangelos Bellos would like to thank “Bodossaki Foundation” for its financial support.

Nomenclature

A_a	Aperture area of the collector, m^2
C	Concentration ratio, -
D	Tube diameter, m
D_W	Distance between reflectors, m
dx	Displacement ratio parameter, -
F	Focal length, m
G_b	Solar direct beam irradiation, W/m^2
K	Total incident angle modifier, -
K_L	Longitudinal incident angle modifier, -
K_m	Mean yearly incident angle modifier, -
K_T	Transversal incident angle modifier, -
L	Concentrator length, m
L_{ext}	Extended length of the receiver, m
L_{sh}	Non-illuminated part of the receiver, m

N	Day duration, h
N_{rf}	Total number of primary reflectors, -
P	Displacement of the receiver, m
SN	Number of the sunny days, -
t	Time, h
W	Total width, m
W_0	Mirror width, m

Greek symbols

α	Absorber absorbance, -
η	Efficiency, -
θ	Solar incident angle, ^{o}
θ_L	Longitude solar incident angle, ^{o}
θ_T	Transversal solar incident angle, ^{o}
λ	Length ratio parameter, -
ρ_1	Primary concentrator reflectance, -
ρ_2	Secondary concentrator reflectance, -
τ	Cover transmittance, -

Subscripts and superscripts

ci	Cover inner
co	Cover outer
day	Mean monthly day
i	Counter of the primary mirrors (i=1…N)
max	Maximum
opt	Optical
ri	Absorber inner
ro	Absorber outer
sec	Secondary

Abbreviations

CPC	Compound Parabolic Concentrator
IAM	Incident Angle Modifier
LFR	Linear Fresnel Reflector
PTC	Parabolic Trough Collector

References

Bellos, E., Mathioulakis, E., Tzivanidis, C., Belessiotis, V., Antonopoulos, K.A., 2016. Experimental and numerical investigation of a linear Fresnel solar collector with flat plate receiver. Energy Conversion and Management 130,44-59.

Bellos, E., Tzivanidis, C., Belessiotis, V., 2017. Daily performance of parabolic trough solar collectors. Solar Energy 158:663-678.

Bellos, E., Tzivanidis, C., Papadopoulos, A., 2018a. Optical and thermal analysis of a linear Fresnel reflector operating with thermal oil, molten salt and liquid sodium. Applied Thermal Engineering 133,70-80.

Bellos, E., Tzivanidis, C., Papadopoulos, A., 2018b. Secondary concentrator optimization of a linear Fresnel reflector using Bezier polynomial parametrization. Solar Energy 171,716-727.

Bellos, E., Tzivanidis, C., Papadopoulos, A., 2018c. Daily, monthly and yearly performance of a linear Fresnel reflector. Solar Energy 173,517-529.

Bellos, E., Tzivanidis, C., Tsimpoukis, D., 2018d. Thermal, hydraulic and exergetic evaluation of a parabolic trough collector operating with thermal oil and molten salt based nanofluids. Energy Conversion and Management 156,388-402.

Bellos, E., Mathioulakis, E., Papanicolaou, E., Belessiotis, V., 2018e. Experimental investigation of the daily performance of an integrated linear Fresnel reflector system. Solar Energy 167,220-230.

Bellos, E., Tzivanidis, C., 2018. Development of analytical expressions for the incident angle modifiers of a linear Fresnel reflector. Solar Energy 173,769-779.

Bellos, E., Tzivanidis, C., 2019. Investigation of a booster secondary reflector for a parabolic trough solar collector. Solar Energy 179,174-185.

Canavarro, D., Chaves, J., Collares-Pereira, M., 2016. A novel Compound Elliptical-type Concentrator for parabolic primaries with tubular receiver. Solar Energy 134,383-391.

Desai, N.B., Bandyopadhyay, S., 2017. Line-focusing concentrating solar collector-based power plants: a review. Clean Techn Environ Policy 19:9.

Gaul, H., Rabl, A., 1980. Incidence-Angle Modifier and Average Optical Efficiency of Parabolic Trough Collectors. ASME. J. Sol. Energy Eng. 102(1),16-21.

Heimsath, A. Bern, G. van Rooyen, D., Nitz, P., 2014. Quantifying Optical Loss Factors of Small Linear Concentrating Collectors for Process Heat Application. Energy Procedia 48,77-86.

Hongn, M., Larsen, S.F., Gea, M., Altamirano, M., 2015. Least square based method for the estimation of the optical end loss of linear Fresnel concentrators. Solar Energy 111,264-276.

Hongn, M., Larsen, S.F., 2018. Hydrothermal model for small-scale linear Fresnel absorbers with non-uniform stepwise solar distribution. Applied Energy 223,329-346.

Huang, F., Li, L., Huang, W., 2014. Optical performance of an azimuth tracking linear Fresnel solar concentrator. Solar Energy 108,1-12.

Kouremenos, D.A., Antonopoulos, K.A., Domazakis, E.D., 1985. Solar radiation correlations for the Athens, Greece, area. Solar Energy 35,259-269.

Loni, R., Kasaeian, A.B., Askari Asli-Ardeh, E., Ghobadian, B., 2016. Optimizing the efficiency of a solar receiver with tubular cylindrical cavity for a solar-powered organic Rankine cycle. Energy 112,1259-1272.

Ma, J., Chang, Z., 2018. Understanding the effects of end-loss on linear Fresnel collectors. IOP Conference Series: Earth and Environmental Science 121,052052.

Manikumar, R., Arasu, A.V., 2014. Heat loss characteristics study of a trapezoidal cavity absorber with and without plate for a linear Fresnel reflector solar concentrator system. Renewable Energy 63,98-108.

Moghimi, M.A., Craig, K.J., Meyer, J.P., 2015. Optimization of a trapezoidal cavity absorber for the Linear Fresnel Reflector. Solar Energy 119,343-361.

Moghimi, M.A., Craig, K.J., Meyer, J.P., 2017. Simulation-based optimisation of a linear Fresnel collector mirror field and receiver for optical, thermal and economic performance. Solar Energy 153,655-678.

Montes, M.J., Abbas, R., Muñoz, M., Muñoz-Antón, J., Martínez-Val, J.M., 2017. Advances in the linear Fresnel single-tube receivers: Hybrid loops with non-evacuated and evacuated receivers. Energy Conversion and Management 49,318-333.

Morin, G., Karl, M., Mertins, M., Selig, M., 2015. Molten Salt as a Heat Transfer Fluid in a Linear Fresnel Collector – Commercial Application Backed by Demonstration. Energy Procedia 69,689-398.

Myers Jr, P.D., Goswami, D.Y., 2016. Thermal energy storage using chloride salts and their eutectics. Applied Thermal Engineering 109B,889-900.

Pulido-Iparraguirre, D., Valenzuela, L., Serrano-Aguilera, J.-J., Fernández-García, A., 2019. Optimized design of a Linear Fresnel reflector for solar process heat applications. Renewable Energy 131,1089-1106.

Qiu, Y., Li, M.-J., Wang, K., Liu, Z.-B., Xue, X.-D., 2017. Aiming strategy optimization for uniform flux distribution in the receiver of a linear Fresnel solar reflector using a multi-objective genetic algorithm. Applied Energy 205,1394-1407.

Qu, W., Wang, R., Hong, H., Sun, J., Jin, H., 2017. Test of a solar parabolic trough collector with rotatable axis tracking. Applied Energy 207, 7-17.

SOLIDWORKS Flow Simulation 2015 Technical Reference

Sun, J., Wang, R., Hong, H., Liu, Q., 2017. An optimized tracking strategy for small-scale double-axis parabolic trough collector. Applied Thermal Engineering 112,1408-1420.

Tiwari, S., Tiwari, G.N., 2016. Thermal analysis of photovoltaic-thermal (PVT) single slope roof integrated greenhouse solar dryer. Solar Energy 138,128-136.

Wang, R., Sun, J., Hong, H., Liu, Q., 2017. An on-site test method for thermal and optical performances of parabolic-trough loop for utility-scale concentrating solar power plant. Solar Energy 153, 142-152.

Yang, M., Zhu, Y., Taylor, R.A., 2018. End losses minimization of linear Fresnel reflectors with a simple, two-axis mechanical tracking system. Energy Conversion and Management 161,284-293.

Zhou, L., Li, X., Zhao, Y., Dai, Y., 2017. Performance assessment of a single/double hybrid effect absorption cooling system driven by linear Fresnel solar collectors with latent thermal storage. Solar Energy 151, 82-94.

Zhu, G., 2013. Development of an analytical optical method for linear Fresnel collectors. Solar Energy 94,240-252.

Zhu, G., Wendelin, T., Wagner, M.J., Kutscher, C., 2014. History, current state, and future of linear Fresnel concentrating solar collectors. Solar Energy 103,639-652.

Zhu, Y., Shi, J., Li, Y., Wang, L., Huang, Q., Xu, G., 2017. Design and thermal performances of a scalable linear Fresnel reflector solar system. Energy Conversion and Management 146,174-181.

Zhu, J., Chen, Z., 2018. Optical design of compact linear fresnel reflector systems. Solar Energy Materials and Solar Cells 176,239-250.